FIRST STREET FOUNDATION

ARUP

First Street Foundation - Arup

Climate Risk and Losses Methodology

Version 1.0

Published: 9/20/2023

Acknowledgements

We would like to thank all collaborators and partners for their support in developing the First Street Foundation Flood Model (FSF-FM), Wind Model (FSF-WM), and Wildfire Model (FSF-WFM) and their associated damages and losses estimates. We are grateful to our partners at Arup, whose expertise is key to the damage, loss, and downtime estimates associated with First Street's peril models. Thank you to members of the Pyrgence Consortium for their contributions to the fire science and expertise in the creation, calibration, and validation of the Wildfire Model. Thank you to the Rhodium Group, a modeling partner dedicated to producing downscaled, bias-corrected climate projection data and tropical cyclone-driven surge data, accounting for current and future climate change, including extreme events. We are also grateful for our partnership with Lightbox, data from which we use to derive property- and building-specific exposure and vulnerability estimates that are key to understanding probable damages and losses. We give a special thank you to our advisory board member, Dr. Kerry Emanuel at the Massachusetts Institute of Technology, for his contributions and feedback. Also, we appreciate all board members and individuals at First Street Foundation who provided time and effort unsparingly.

FIRST STREET FOUNDATION

Table of Contents

Executive Summary

Estimates of the economic impacts of climate risk exposure have been created through a partnership between the science nonprofit First Street Foundation and the international engineering firm Arup Corporation. These estimates leverage the scientific property-specific, climate-adjusted measures of environmental risk from flood, wildfire, and wind exposure created by First Street with the engineering expertise of Arup to discern the likely repair and replacement costs, as well as expected downtime for impacted structures on all properties across the US. The scientific methodologies for risk have been developed and published using open science by First Street, who as a nonprofit organization has made them openly available and subjected them to scientific peer-review. Arup has used their proprietary, first-principles-of-engineering methods to provide the likely repair/replacement costs and downtime for each property given First Street's estimates of hazard exposure and specific building characteristics. Arup's knowledge and expertise is captured in a set of fragility curves that they have created for each peril, and for many dozens of building archetypes. These archetype and peril-specific curves relate the likely damage or downtime to be experienced by a building of that type when exposed to a peril of a particular severity (e.g. water depth for flood, flame length for wildfire). The costs and downtimes resulting from each building's assessment of its vulnerability and exposure are combined with a RiskFactor™ score for each US property and made publicly available for noncommercial purposes at RiskFactor.com to enable every American to begin to understand how climate change and environmental risk are impacting their homes and businesses today, as well as 30 years into the future. These loss estimates are key to making environmental change personally relevant to a wide audience, and to enable well-informed decisions in a changing climate.

1. Flood

First Street Foundation has created a probabilistic flood exposure model, the First Street Foundation Flood Model (FSF-FM), that describes compound flood risk under a range of possible current and future climate conditions in the United States (Porter et al., 2023; Wing et al., 2022). The FSF-FM is a national, property-specific flood model that utilizes well-established hydraulic models (Bates et al., 2021), with inputs from international climate model results and novel analyses of changing rainfall characteristics across the US to enable probabilistic projections of flood risk 30 years into the future (Kim et al., 2022). An economic loss model has been built upon the FSF-FM, utilizing the Arup Corporation's engineering expertise. The Arup's loss modeling approach simulates the impact of hundreds or thousands of different flooding scenarios using a virtual model of the building type to estimate the extent and severity of flood damage on individual building components and translates it to consequences such as financial loss and downtime. This loss modeling approach has enabled assessments of National, regional, state, and local flood risk (e.g., First Street's National reports on Climate-driven flood risk, Precipitation and Climate Change, Commercial flood impacts, Community infrastructure risks) and its implications for communities, real estate values, and populations across the US (Porter et al., 2021; Wobus et al., 2021; Gourevitch et al, 2023; Flores et al., 2023; Shu et al., 2022; Wing et al., 2022; Armal et al, 2020; Tedesco, et al., 2020; McAlpine and Porter, 2018).

Arup developed vulnerability curves in conjunction with the First Street Foundation in order to relate flood depth to financial loss or downtime for thirty building archetypes representing commercial office, retail, and multi-unit residential spaces of various heights, construction material, and basement configurations. Each archetype model was populated with typical building components including structural members, equipment, plumbing, electrical lines, partitions, and finishes according to building properties such as area, height, and usage. The vulnerability curves were derived by the approach outlined below.

Structural Damage Impacts

Within any building, the probability that individual components would sustain a certain severity of damage (from minor or repairable damage to full replacement) for a given flood depth is defined by fragility curves. These component-based fragility curves were developed by Arup based on first principles of engineering, observations from field reconnaissance in the aftermath of past flood events (e.g. Hurricane Harvey), other guidelines (e.g. NEMA Ingress Protection standards), or adapted from the engineering and scientific literature. Figure F1 shows an example family of fragility curves for interior partitions, where DS1 (blue line) refers to partial failure of the partitions (which requires replacement of at least the bottom 4 ft of drywall panel) and DS2 (red line) represents complete failure of the partitions (which requires full replacement from floor to ceiling).

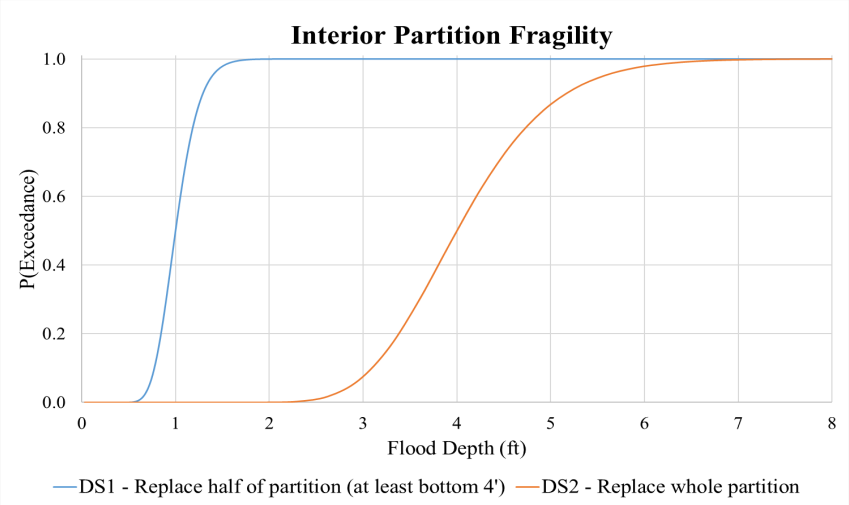

Figure F1. Fragility curves for interior building partitions. DS1 (blue line) refers to partial failure of the partitions and DS2 (red line) represents complete failure of the partitions.

Each building model, populated with components arranged according to its size and archetype, was subjected to incremental flood depths from one foot up to fifteen feet. For each flood depth, one thousand Monte Carlo simulations were run, sampling the fragilities of each component so that component-level damage results were produced for each of the 1,000 realizations. This modeling approach captures the inherent variability in flood impacts and quantifies the bands of uncertainty.

Arup developed this component-based approach for flood risk analysis based on a methodology that was originally used to quantify seismic risk, adopted from FEMA P-58 (Applied Technology Council, 2013) and enhanced to more realistically capture building downtime with Arup's

Resilience-based Earthquake Design Initiative (REDi) methodology (Arup, 2013). In the past several years, Arup has adapted this seismic component-level approach to climate-related hazards. Recently, academic researchers have also been adapting this type of approach for flood risk modeling (Nofal & van de Lindt, 2020).

From these damage results, the number of units for each component needing to be repaired or replaced (according to its damage state) were obtained for each simulation. This information was used for the financial loss and downtime calculations. Arup also developed consequence functions that link each damage state defined in the fragility curves to specific levels of financial loss and lengths of repair times, based on data procured by Arup's cost estimators. The costs to repair and replace equipment were estimated for Washington, DC in 2020 USD. Based on the level of damage, the total building financial loss was calculated for each realization as a sum across all damaged components. The estimates produced through the Washington D.C. baseline application were then adjusted to be appropriate for each of the other geographical locations through the use of price parity multipliers from the Bureau of Economic Analysis (BEA) by Metro area (CBSA), or state, for counties outside of metro areas. Structural damage impacts are calculated for the three categories of retail, office, and multi-unit residential buildings as these archetypes are appropriate for application to these types of large buildings and multi-unit residential properties serve as an important source of revenue for building owners.

Downtime Impacts

Downtime estimates are directly related to structural damage and are calculated through the additional inclusion of the aggregated repair time per damaged component in the building and impeding delays as they relate directly to normative locations of building infrastructure and local market conditions associated with the availability of construction/repair labor following the modeled flood event. The downtime calculation also followed Arup's aforementioned REDi methodology. Overall, the process for the calculation of downtime estimates follows a similar process as that for structural damage estimates.

For downtime estimates, rather than information on the cost of replacement for each component to

estimate monetary loss, information regarding the repair times for damaged components and impeding factors that delay the initiation of building repairs are utilized to calculate time. Impeding delays include time for floodwater recession, building restoration, contractor and engineer mobilization, and equipment long lead times. Once the impending delays are resolved, the downtime model allocates crews of workers to make repairs to damaged components based on specific trades (e.g. electrical). A construction of realistic repair sequences that mimic actual contractor logistics is aggregated to quantify the overall building downtime. As a result, downtime impact estimates also rely on the calculation of property-specific structural damage costs and is estimated utilizing information regarding the 3 percentile-based values (10th, 50th, and 90th percentiles) of downtime per flood depth for each of the 30 different building archetypes coupled with the property's hazard and exposure information. Where possible, these results were compared to literature as a benchmarking exercise (FEMA, 2020) (U.S. Army Corps of Engineers, 2009) (Nofal & van de Lindt, 2020).

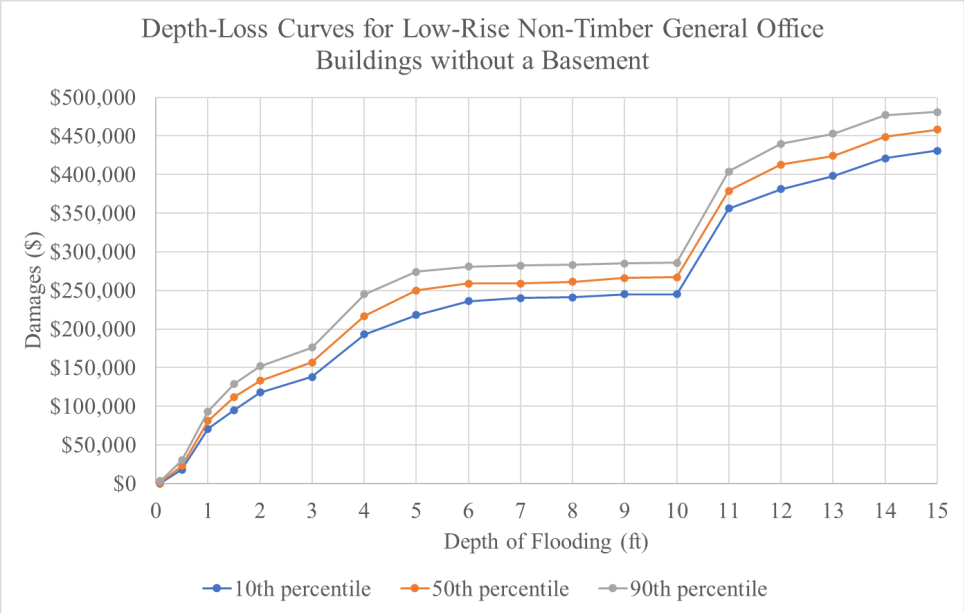

Figure F2. Low-rise Office building (non-timber) building archetype vulnerability curve for the 10th, 50th, and 90th percentile losses

Economic Impacts

Finally, economic impacts (direct and indirect) from retail and office buildings are estimated as indicators in the reduction of outputs and other associated economic activity due to downtime, and are calculated through the inclusion of information on land-use, geographic location, square footage, GDP contribution by sector, and RIMS II multipliers capturing indirect market-level impacts (https://apps.bea.gov/regional/rims/rimsii/home.aspx). Economic impacts refer to the economic losses incurred due to retail and office buildings being closed from flooding. This includes direct economic losses from economic activity not occurring that would normally occur in the impacted building due to the estimated downtime (detailed above). Additionally, indirect impacts (also referred to as flow or downstream effects) are partially captured here through the application of state and sector specific economic multipliers provided by the BEA RIMS II. These indirect impacts refer to the foregone economic activity in the region due to the direct economic impacts. For example, an office building which normally purchases large amounts of office supplies but which now has interrupted operations due to flooding results in indirect impacts due to this foregone market activity where it is not engaging in the purchase of those supplies during downtime. More broadly, indirect impacts result when a flooded building cannot operate as a supplier for outputs, or cannot operate as a buyer during downtime.

The model for estimating these economic impacts utilizes three sets of input data: (1) state and county-level GDP information identifying contributions by different economic sectors, (2) mappings between economic sectors and land uses, and (3) economic multipliers by state and sector. These data sets are sourced from the BEA, First Street Foundation (FSF), and the BEA RIMS II, respectively. In order to link the existing parcel data to BEA-RIMS industry sectors, BEA data is mapped to a land use category consistent with the land use types included in the archetype development. The sector GDP data is summarized by land use to give “land use GDP”, or the economic contribution of a given land use category by state and county.

Next, the property database is used to generate total building square footage for buildings with retail and office land uses. The “land use GDP” is divided by the total square footage per land use to compute the expected land use GDP-per-sqft for each land use category by state and county. For each retail and office property with flooding, the estimated downtime, the building square footage is multiplied by the expected land use GDP-per-sqft. This is the property’s direct economic

losses. A deflator is used which assumes only 40% of activity decreases, as people may be able to work from home. It is also important to note that since the GDP information is provided on a state or county resolution and GDP for the land use categories involve the aggregation of multiple sectors, direct economic losses will not be an accurate portrayal of individual properties but should be considered only on a larger geographical scale, or labor market level.

Indirect losses are calculated by multiplying the direct losses by a land use multiplier, which is computed through utilizing the RIMS sector multipliers. These indirect losses account for economic activity like lost output, lost value, lost household earnings, and lost jobs (BEA, 2012). As the sectors used in the RIMS multipliers are much more specific than the land use categories utilized in the property data here (office and retail), a “land use multiplier” is computed for each of the two categories by taking a weighted average of each sector included within each land use category, based on the ratio of each included sector’s contribution to GDP. This is done individually for each state.

The RIMS II multipliers for each state and sector exist as type 1 and type 2, where the type 2 multipliers not only consider the downstream impacts of foregone macro-level market transactions but also the impacts of foregone purchases due to employees' income being reduced from their place of work being closed. A key assumption utilized here is the appropriateness of the RIMS II type 1 multipliers over the type 2 multipliers. The type 1 multipliers were utilized as it was assumed that employee income and purchasing power would not be reduced. This relies on an additional assumption that most employees receive incomes through salary rather than hourly pay. Additionally, this supports that some employees may be able to work from home during downtime. When considering retail buildings such as restaurants where employees are more likely to be employed on an hourly basis and cannot as often work from home, this presents an obvious opportunity for model improvement when this type of high resolution data is available.

2. Wildfire

A novel risk modeling approach was developed to evaluate wildfire risk to residential, commercial, and industrial buildings across the United States, resulting from a collaboration of the fire science experts at the Pyregence Consortium, First Street, and Arup. Others' currently available approaches to this problem are either qualitative in nature, regional in scale, or developed based on historical losses which limit applicability to predictive models. The First Street Foundation Wildfire Model (FSF-WFM) was developed using a wildfire behavior model run as a Monte Carlo simulation to describe the burn probability, likely flame length, and ember characteristics for all possible wildfires today, and across the US for 30 years into the future (Kearns et al., 2022). The resulting statistical descriptions of wildfire exposure are useful in evaluating climate-driven wildfire risk at a property level (see First Street's assessment of Wildfire risk) and can also be used to examine smoke exposure (Melecio-Vázquez et al., 2023).

Arup addressed an industry-wide gap in the quantification of wildfire risk by developing component-based fragility models which translate wildfire intensity to ignition probability of a structure, thereby characterizing the vulnerability of a given building based on its characteristics. The model is underpinned by first principles of engineering, including heat transfer mechanics, which allowed Arup to develop a library of fragilities for typical building components of different materials and assemble them into building archetypes. When paired with First Street Foundation's wildfire hazard model, the fragilities are used to estimate the extent and severity of potential fire damage to the building. Ultimately, the damage can be translated to consequences such as financial loss and downtime to recovery.

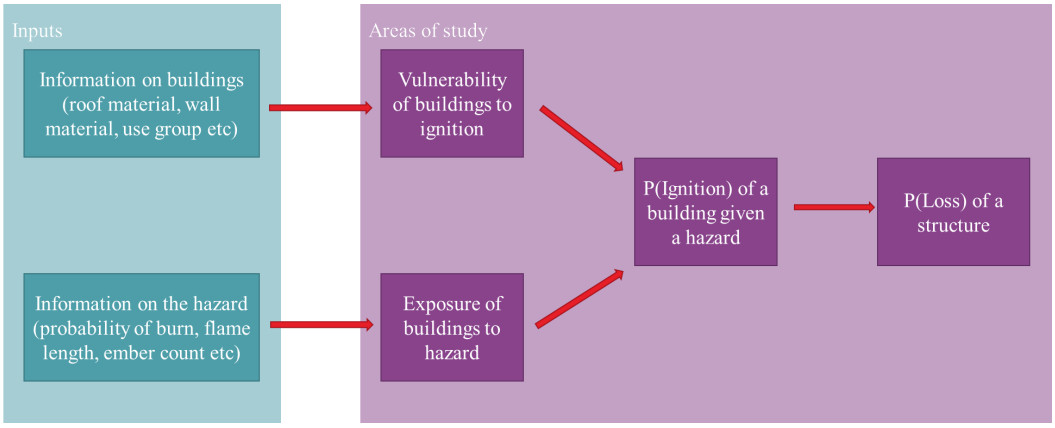

Figure WF1: Overview of the risk modeling methodology.

Exposure

Arup defined 72 building archetypes to characterize the building stock exposed to wildfire hazard, covering residential, commercial, and industrial buildings in the United States. We used data provided by First Street Foundation on building characteristics and surrounding vegetation (e.g. a measure of the “defensible space” without vegetation around a building) to categorize building vulnerability and develop the archetypal models. The included characteristics represent the key aspects that contribute to structure ignition probability and the consequences of wildfire events. These characteristics include building use, external envelope materials (external wall and roof materials), height, defensible space, and compliance with applicable wildfire codes and standards. See Table WF1 for a descriptive list.

Characteristic	**Categories**
Use Type	• Residential • Commercial • Industrial
Roof Material	• High ignition potential / combustible • Low ignition potential / combustible • Non-combustible
Exterior Wall Material	• High ignition potential / combustible • Low ignition potential / combustible • Non-combustible
Height	• High-rise • Not high-rise
Defensible Space	• Significant space / little to no shrub coverage • No space / significant shrub coverage
Code Status	• Built before local wildfire code was adopted / does not comply with the wildfire code • Built after local wildfire code was adopted / complies with the wildfire code

Table WF1: List of characteristics used to define and model building archetypes.

Vulnerability

The Figure WF2 below depicts key considerations in the component-based building archetype models.

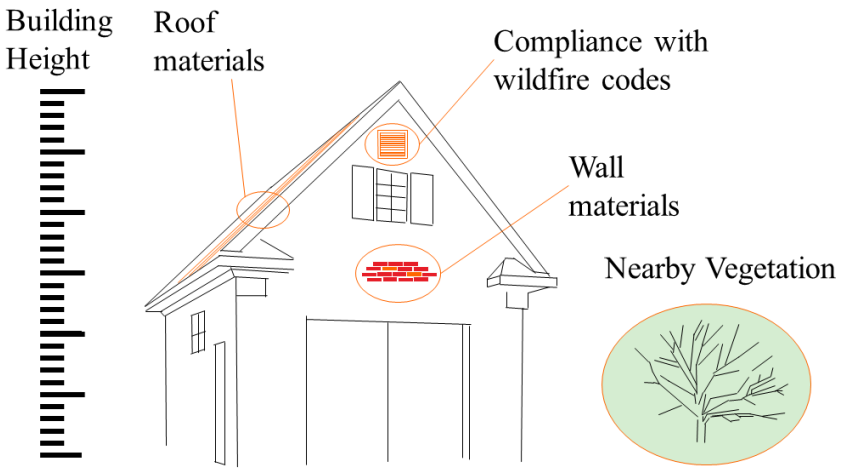

Figure WF2: Key aspects of the construction considered for wildfire-driven losses.

Arup modeled the likelihood of ignition for a building exposed to several hazards from a wildfire, including:

- Direct flame impingement on the building from the fire,
- Radiative heat transfer from the fire to the building,
- External collections of embers within the envelope of the building, and
- Embers which enter the building.

Evidence from past fires indicates that embers are the leading cause of ignition (Nazare et al., 2021; Blanchi and Leonard, 2005). The key components of the wildfire hazards are summarized in Figure WF3 below.

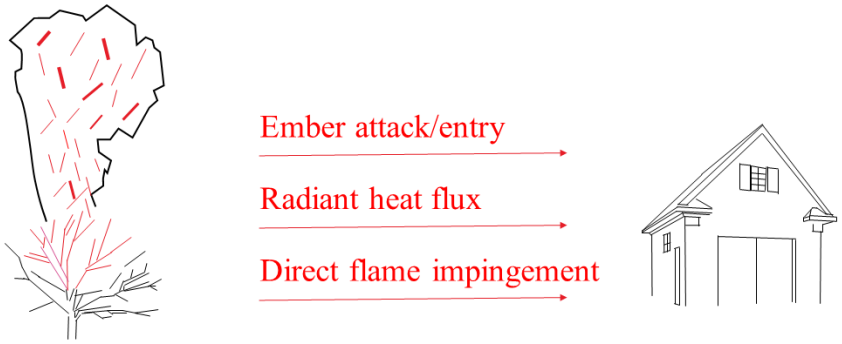

Figure WF3: Key hazards to buildings from wildfire.

For each archetype building, the vulnerability model determined the probability of ignition from (1) the flame front and (2) ember attack. See the sub-sections below for additional details.

Flame Front

Ignition from the flame front uses the flame length output from the wildfire hazard model and distance to the structure to quantify the heat flux experienced by the building envelope materials. The analysis considered both direct flame impingement and radiative heat transfer from the flame to the building. The vulnerability of external envelope materials was modeled by Arup using the principles of heat transfer and ignition.

Ignition from the flame front is highly dependent on the distance between the flame front and the building. This distance was determined by employing Monte Carlo simulations to account for uncertainty in the locations of the flame front and building, which is limited by the resolution of the First Street wildfire hazard model, which discretizes the landscape in 30x30 meter (~100x100 ft) pixels. Ignition of the building envelope materials was modeled by using standard quantification of incident radiative heat flux. Flame length in the pixel (or adjacent pixel), which is the output of the wildfire hazard model, and the width of the pixel were used to define the size of the emitter for this calculation. The incident heat flux was then calculated based on the fire intensity, emissivity, view factor, distance from the flame front etc. (NFPA, 2002; Penney et al., 2020). The threshold for ignition of the building envelope materials (i.e. exterior wall and roof) were determined from

duration dependent critical heat flux values from literature (Babrauskas and SFPE, 2003). This calculation was performed as a Monte Carlo simulation to account for the fact that there is a range of plausible heat flux ignition thresholds within each combustibility category. The result for each building category is a fragility curve relating the probability of ignition to heat flux experienced by the building (see Figure WF4 below).

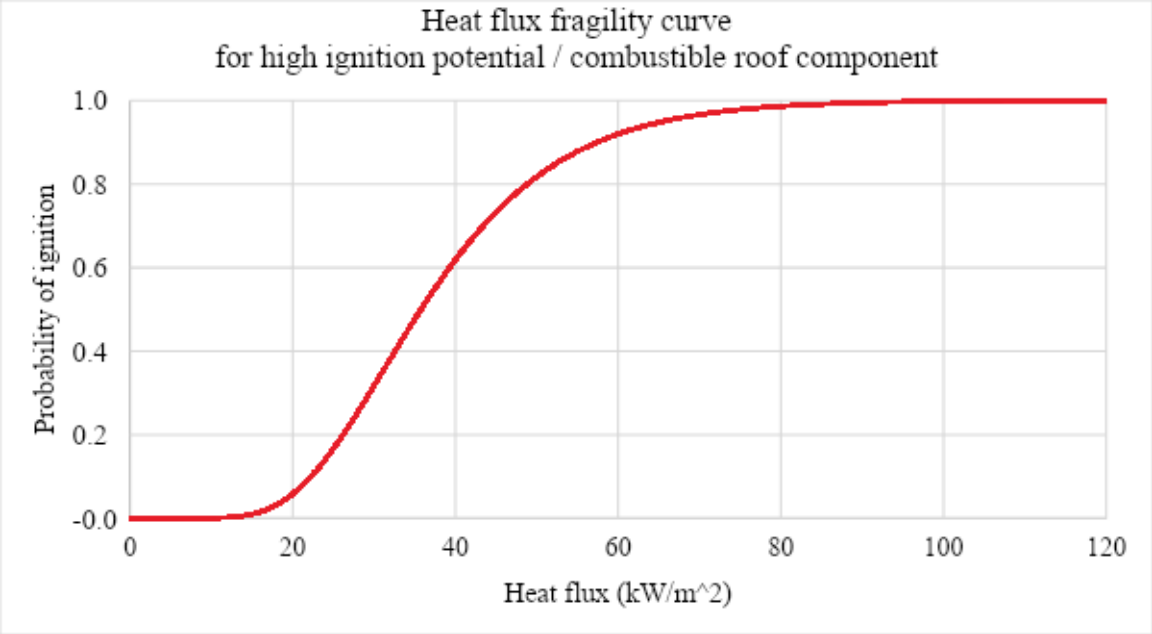

Figure WF4: Probability of ignition versus calculated heat flux for the high ignition potential / combustible roof component.

Ember Attack

To model the probability of ignition from ember attack (i.e. exposure to ember wash from firebrands expelled by a wildfire and cast downwind), the analysis considered both internal ignition from embers which enter the building via openings and vents, and external ignition from embers which land or collect on the building envelope materials. In each simulated wildfire, the density of embers landing in each pixel in which a building is located was calculated based on data provided by the wildfire hazard model. The data was calibrated based on observations of ember density in past wildfires and experiments, as well as a review of the wildfire hazard simulations – specifically the wildfire area and number of embers generated in each wildfire, from both observations of opportunity (Rissel and Ridenour, 2014; Foote et al., 2012) and experimental results (Thomas et al., 2017; Zen et al., 2021; Filkov and Prohanov, 2019).

Monte Carlo simulations were performed by Arup to estimate the number of embers entering the building via openings and vents. These simulations accounted for uncertainty in the ember density into the pixel (given the wildfire hazard model results) and uncertainty in what proportion of embers landing in the pixel would enter the building through opening and vents. The results depend on the code status of the building, which dictates the porosity of vents and openings.

Monte Carlo simulations were also performed to estimate the number of embers landing and collecting on the roof of the building. Similar to the simulations performed to estimate the number of embers entering the building, these simulations accounted for uncertainty in the ember density into the pixel and uncertainty in what proportion of embers landing in the pixel would land and collect on the roof. The likelihood of ignition from this collection of embers was determined as a factor of the number of embers in the pile, a characteristic exposure from the pile (e.g. heat transfer intensity and duration), and the critical heat flux of the building envelope materials. The overall likelihood of ignition from ember attack was calculated as the union of these separate mechanisms.

Losses

To model consequences of each hazard intensity in the vulnerability model, damage data from past wildfires (Government Operations Agency, 2022; State of California-Cal Fire, 2022; Wallingford, 2018) was reviewed and three damage states were developed: Total Loss, Major Damage, and Not Ignited. The review of past wildfires, including the Camp Fire (2018) and Tubbs Fire (2017), showed significant differences in impact to buildings that were ignited versus not ignited, and this review indicated that if a given building had ignited, the resulting damage state was almost always total loss, with some likelihood of the building experiencing major damage, depending on the archetype. Complete destruction, or total loss, can be prevented by building-specific firefighting activities during the event, but these efforts are difficult to ascertain a priori and were not considered in the model.

For each of these damage states, the financial loss and downtime were estimated using building-level loss curves. These loss distributions were developed from literature review of previous wildfire events (see Appendix WFA for a listing of these sources).The financial loss values were determined as a percent of replacement cost, which assumed full reconstruction. Replacement costs were estimated by the Arup team for detailed use types based on project experience. These were anchored in 2021 USD for Sacramento, California. The costs were provided to First Street Foundation to be scaled to local market conditions in other locations across the United States using BEA price parity multipliers by Metro area, county, or state designation, in an approach similar to that taken for Flood losses. The downtime estimates incorporated the time it takes for occupants to evacuate and later return, for crews to fight the fire and clear debris, for owners to address any immediate safety concerns before reoccupation (even if unignited), and for financing and conducting the repairs or reconstruction if required.

For each of the building archetypes, Arup provided the average financial loss and average downtime caused by either flame length or ember count. These loss curves, when appropriately combined with the likelihood, intensity, and source of wildfire hazard at a site (due to flame front and/or embers), can be used to estimate the average annual loss (AAL) for each building. Figure WF5 provides an example loss curve for a residential building archetype with high ignition potential / combustible wall, low ignition potential / combustible roof, and no defensible space, subject to

wildfires of a given flame length.

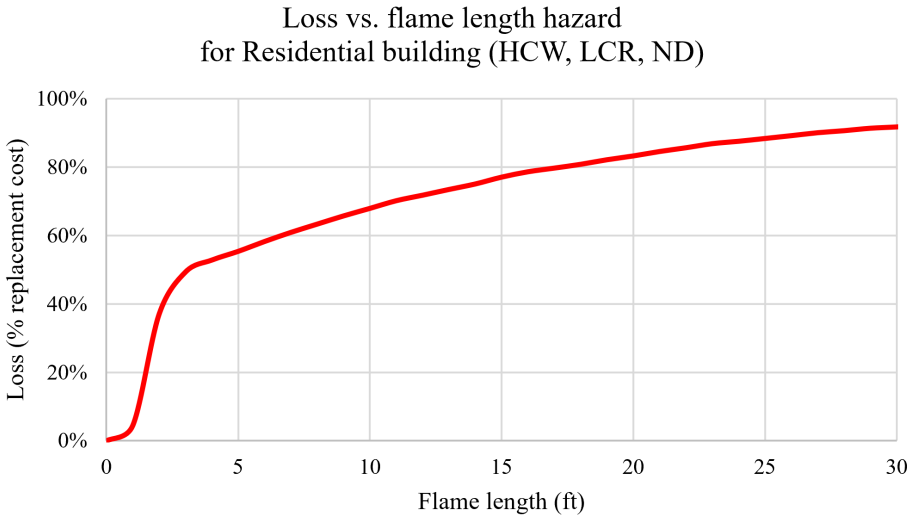

Figure WF5: Loss as percent replacement cost for incremental modeled flame length for one residential building archetype (HCW=high ignition potential / combustible wall, LCR=low ignition potential / combustible roof, ND=no defensible space).

This novel risk modeling approach integrated probabilistic wildfire hazard data across the United States, characterization of critical building vulnerabilities based on first principles of engineering and physics, and propagation of uncertainty throughout the loss modeling. For the first time, the probability of building ignition from wildfires and the resulting losses and downtime have been quantified using an engineering-based methodology and used to develop a better understanding of wildfire risk across the country and for individual properties.

Appendix WFA: Studies of fire damages used for losses estimation

Published research results, wildfire reports and and incident assessments used in the determination of losses from wildfire events include:

1. National Institute of Science and Technology (NIST) case study data, including reports for Witch / Guejito Fires (2007), Willow Creek / Tanglewood Fires (2011), Waldo Canyon Fire (2012), and Camp Fire (2018).
    a. Maranghides, A.; McNamara, D.; Mell, W.; Trook, J.; & Toman, B. (2013). A case study of a community affected by the Witch and Guejito Fires Report (NIST Technical Note 1796). NIST, U.S. Department of Commerce. Retrieved from http://dx.doi.org/10.6028/NIST.TN.1796.
    b. Maranghides, A.; McNamara, D.; Vihnanek, R.; Restaino, J.; and Leland, C. (2015). A case study of a community affected by the Waldo Fire (NIST Technical Note 1910). NIST, U.S. Department of Commerce. Retrieved from http://dx.doi.org/10.6028/NIST.TN.1910.
    c. Maranghides, A.; and McNamara, D. (2016). 2011 Wildland Urban Interface Amarillo Fires Report #2 (NIST Technical Note 1909). NIST, U.S. Department of Commerce. Retrieved from http://dx.doi.org/10.6028/NIST.TN.1909.
    d. Maranghides, A.; Mell, W.; Hawks, S.; Wilson, M.; Brewer, W.; Link, E.; Brown, C.; Murrill, C.; and Ashley, E. (2020). Preliminary data collected from the Camp Fire reconnaissance (NIST Technical Note 2128). NIST, U.S. Department of Commerce. Retrieved from https://doi.org/10.6028/NIST.TN.2128.

2. County-level reports and local news articles covering various wildfires.
    a. Chandler, M. (2019, July 26). Carr Fire recovery, 1 year later: Why hundreds of homes still haven't been rebuilt. Record Searchlight. Retrieved from www.redding.com.
    b. Kasler, D. and Reese, P. (2019, April 11). In Camp Fire, newer houses were much less damaged. KQED. Retrieved from www.kqed.org.
    c. McGough, M. (2021, Sept 14). California wildfires: Caldor Fire damage inspection complete; Dixie Fire near million acres. The Sacramento Bee. Retrieved from

www.sacbee.com.

d. McKay, J. (2020, Nov. 18). After Camp Fire, Paradise, CA works on long-term recovery. Government Technology. Retrieved from www.govtech.com.
e. Newboles, A. (2020, Sept 27). Cal Fire releases final North Complex damage totals in Butte County. KRCR. Retrieved from krcrtv.com.
f. Orbital Insight. (2019, Oct 15). Measuring impact and recovery of California wildfires. Retrieved from orbitalinsight.com.
g. Solano County. (2020). LNU Lightning Complex Fire. Solano County Office of Emergency Services. Retrieved from www.solanocounty.com.

3. Journal articles and resources about preparation for and recovery from wildfires.
    a. Alexandre, P.M.; Mockrin, M.H.; Stewart, S.I.; Hammer, R.B.; and Radeloff, V.C. (2015). Rebuilding and new housing development after wildfire. International Journal of Wildland Fire, 24, 138-149. Retrieved from www.fs.fed.us/rm.
    b. CA State Senate Committee on Insurance. (2021, March 11). Informational Hearing – Wildfires and Insurance: Emerging Issues. California State Senate. Retrieved from sins.senate.ca.gov.
    c. CAL FIRE. (2019). Before, during and after a wildfire. Retrieved from www.fire.ca.gov.
    d. CAL FIRE. (2019). Post-wildfire recovery. Retrieved from www.readyforwildfire.org.
    e. CAL FIRE. (2019). Returning home after a wildfire. Retrieved from www.readyforwildfire.org.
    f. Knapp, E.; Valachovic, Y.S.; Quarles, S.L.; and Johnson, N.G. (2021). Factors associated with single-family home survival in the 2018 Camp Fire, California (preprint). Retrieved from https://doi.org/10.21203/rs.3.rs-580864/v1.
    g. Sommer, L. (2020, Nov 25). Rebuilding after a wildfire?. NPR. Retrieved from www.npr.org.

3. Tropical Cyclone Wind

The climate risk modeling approach taken by First Street for tropical cyclone wind provides exposure estimates via the First Street Foundation Wind Model (FSF-WM) through the application of synthetic current and future tropical storm tracks that have been adjusted for climate change impacts (Emanuel et al., 2006) and used to generate hazards used for assessments of wind risk to US properties. These probabilistic hazard estimates feed Arup's simulation of the impact of hundreds or thousands of different hurricane scenarios using a virtual model of the building to estimate the extent and severity of hurricane damage on individual building components and translates those to consequences such as financial loss and downtime. Following this risk modeling approach, a series of curves reflecting downtime and financial loss from wind events were developed for a suite of building archetypes. A rigorous simulation-based methodology was used by Arup to develop these curves. The following discusses how the archetypes were determined and the methodology for developing the curves.

Archetype Development

A set of 30 non-residential and 26 residential archetypes were developed by Arup and selected for assessment. The following key building characteristics were considered: Building occupancy (e.g., industrial, commercial, residential), number of stories, roof material (concrete topping or non-concrete topping roof), missile environment (high or low), and design wind speed zone (this determines the envelope component wind resistance). These are the most critical building characteristics that will affect both building performance during damaging wind events as well as the associated financial loss and downtime (FEMA, 2000). These characteristics are also selected based on the availability of First Street Foundation building data inventory. Based on the building inventory data First Street Foundation provided, the range of each characteristic was selected to best cover the building stock data. The archetypes were developed considering the practical and possible combinations of these different characteristics.

Risk Modeling

The risk modeling approach simulates the impact of wind scenarios using a virtual model of the building to estimate the extent and severity of wind damage on individual building components and translates it to consequences such as financial loss and downtime. Arup developed this component-based approach for wind risk analysis based on a methodology that was originally used to quantify seismic risk, adopted from FEMA P-58 (Applied Technology Council, 2013) and enhanced to more realistically capture building downtime with Arup's Resilience-based Earthquake Design Initiative (REDi) methodology (Arup, 2013). As noted in descriptions for Flood and Wildfire losses, Arup has adapted this seismic component-level approach to several climate-related hazards.

Damage simulation

The building models were populated with typical building components that could be damaged in wind events. During an actual wind event, how a given building component is impacted depends on the location of the component, the orientation of the component, the interaction with other components, the wind resisting capacity of the component, etc. These complexities were explicitly captured by creating a 3D physical based simulation model for each building archetype. The simulation procedure developed captures the following key features:

- Component location, orientation, and the geometry effect of wind pressure
- Progressive failure behavior of components and interaction between components
- Updates to the internal pressure due to envelope component breach
- Wind-driven rain damage due to envelope breach
- Uncertainty of wind pressures and wind resisting capacities

The general procedure considered for damage simulation is consistent with the state-of-art methods in the field (FEMA 2000, FPHLM 2015, Abdelhady et al. 2021, Alduse et al. 2022).

3D wind damage simulation model

For each building archetype, the envelope building components are included explicitly in a 3D model. For each wind event simulated, the pressure load on each individual component was calculated based on the wind direction, component geometry, location, and other characteristics. The pressure load on each component was compared with the component's wind resistance. Failure was determined when the pressure load/uplift force on one unit is larger than the capacity of the associated failure mechanism. Figure TCW1 shows an example of a damage assessment for a typical residential wall component and typical commercial roof component. This process was conducted for each component unit modeled for each archetype.

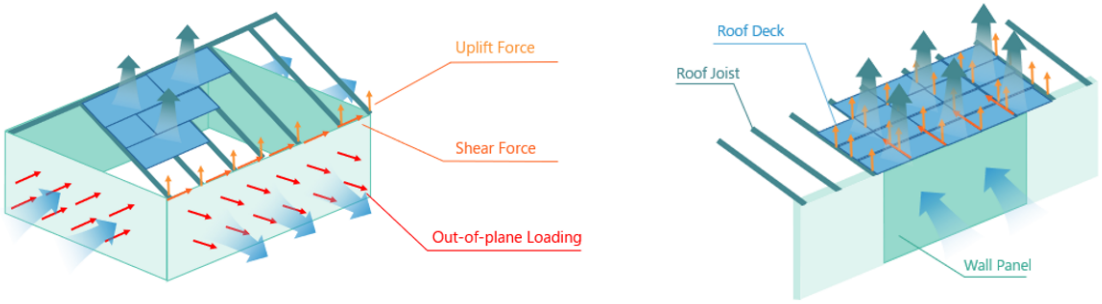

Figure TCW1: Illustration of wind demand calculation for the 3D damage model. Left: residential building wall calculation. Right: commercial building roof calculation

For all archetypes other than single family residential buildings, the envelope components included were windows, doors, roller doors, roof cover, roof deck, roof joist, wall panels, rooftop equipment (e.g., cooling equipment for the HVAC system), and exterior ground equipment (e.g., transformers). Note that not all components were included in the model for every archetype. For the single-family house archetypes, the building envelope components included were windows, doors, garage doors, roof cover, roof sheathing, roof trusses, and wall panels. Each unit of the component type is assigned in a 3D building geometry model based on assumed distribution and quantity.

Wind pressure calculation

The wind pressure is calculated based on the wind speed, wind direction and the wind pressure coefficients following general procedures described in ASCE 7-22 (ASCE 22). The external pressure coefficients are a function of the location of the component unit and the direction of the wind. For each individual component unit considered in the 3D model, the location zone was assigned. The corresponding pressure coefficient for the location zone was selected for the calculation. These pressure coefficients were obtained from Banik et al. (2017), which were derived from past wind tunnel tests.

Wind resisting capacity

The wind resisting capacity for each failure mechanism for each component is explicitly assigned for each archetype. For non-single-family archetypes, it is assumed that the components are designed to fulfill code requirements based on the design wind speed, and the capacity of each component was calculated accordingly. Three levels of building component capacities were considered for different archetypes (100 mph, 125 mph, and 160 mph design wind speed for low, medium, and high wind zones, respectively). For single family archetypes, the component capacities are determined based on available literature data (FEMA 2000, FLPHM 2015). The capacity is also updated dynamically through the simulation. For example, when a given connection fails, the capacity will be reduced for the adjacent component.

Rain intrusion damage

During a hurricane event, rain intrusion could occur through the damaged envelope components. 24-hour rainfall amounts were obtained based on the relation developed by Pita et al. (2012). The amount of rain entering each floor is explicitly calculated based on the breach area of the roof and/or side envelope of the building (see Figure TCW2 for a schematic of a breach). The interior damage percentage was estimated based on the water depth following the relation in Hazus (FEMA 2000). The interior damage percentage was used in the consequence calculation to estimate the cost and downtime due to interior rain damage.

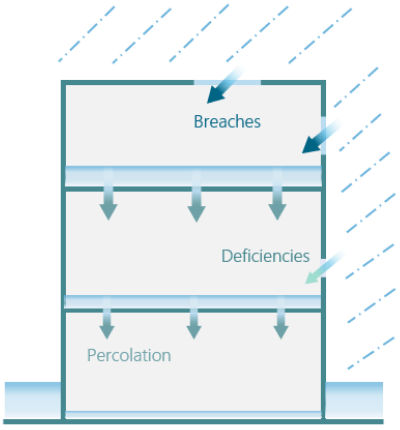

Figure TCW2: Illustration of rain intrusion calculation following breach

Treatment of uncertainty

To account for the uncertainty involved in the simulation process, the damage simulation for each wind event was repeated 500 times. A Monte Carlo simulation procedure was used to sample the capacity for each individual component unit from the predefined distributions and to account for the uncertainty in the components wind resistant capacities. The wind pressure coefficient on each component was also sampled for each realization. Note the sampling was conducted independently for each individual component unit assessment. The distribution parameters used followed the recommendation in Vickery et al. (2006).

Consequence Assessment

Each building archetype was subjected to wind speeds ranging from 30 mph to 200 mph in 10 mph increments and 8 different wind directions. For each wind speed and direction, 500 Monte Carlo simulations were run. Detailed component damage results were produced based on the damage simulation procedure discussed above for each of the 500 realizations. From the damage results, the number of units for each component needing to be repaired or replaced (according to its damage state) were obtained. This information was used for the financial loss and downtime calculations. Arup also developed consequence functions that link each component damage state to specific levels of financial loss and lengths of repair times. Based on the damage results, the consequence assessment was conducted to obtain the financial loss and downtime.

Financial loss

Financial loss values (i.e., the cost to repair or replace a component) were based on data procured by Arup's cost estimators. These costs were estimated for Washington, DC in 2022 USD. To get accurate financial loss estimates for other regions, First Street Foundation scales the financial losses using an appropriate metro area location factor from regional price parity data from the Bureau of Economic Analysis. Based on the level of damage, the total building financial loss was calculated for each realization as a sum across all damaged components. Financial loss values are reported as average loss per square foot.

Downtime

The downtime calculation followed the REDi methodology, which was originally published in REDi for Seismic (Arup, 2013) and adapted for wind by Arup. Downtime consists of repair times for damaged components and impeding factors that delay the initiation of building repairs. Impeding delays include time for returning from evacuation, building restoration, contractor and engineer mobilization, and equipment long lead times. Once the impeding delays are resolved, the downtime model allocates crews of workers to make repairs to damaged components based on specific trades (e.g., structural or building envelope). A construction of realistic repair sequences that mimic actual contractor logistics is aggregated to quantify the overall building downtime

Loss Curves

Once the downtime and financial loss have been calculated for each realization and for each wind speed and wind direction, a set of loss curves (financial loss vs wind speed, downtime vs wind speed) for all archetypes were calculated and provided to First Street. Downtime and financial loss curves, representing the 10^{th}, 50^{th} (median), and 90^{th} percentiles of the results were calculated (see Figure TCW3 for an example).

Where possible, the loss ratios were compared against the Hazus hurricane model for similar archetypes as a benchmarking exercise (FEMA 2000). There was general agreement between Hazus and the models developed in this study on the wind speed thresholds where a significant increase in the building loss ratio is observed. Note that the archetype definitions, the damage and consequence modeling assumptions are different compared to Hazus, so the benchmark aims to

seek agreement on rough range of wind speeds observed.

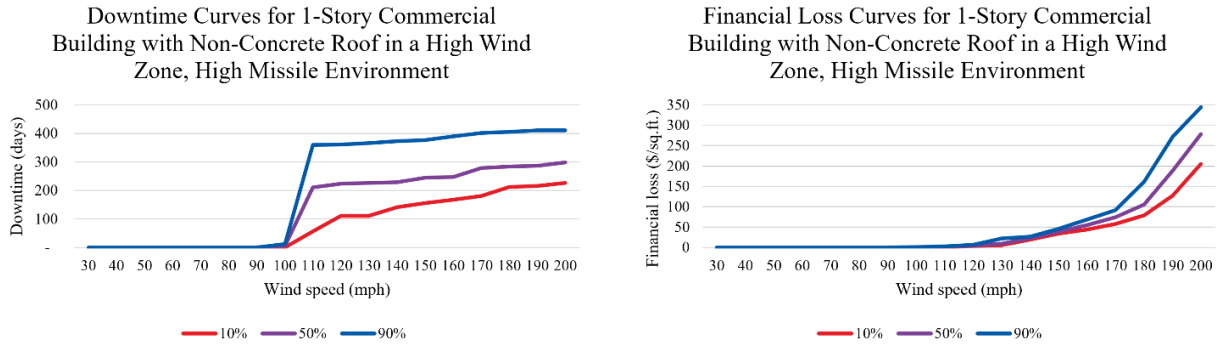

Figure TCW3. Loss curves for a 1-story commercial building with a non-concrete roof in a high wind zone, high missile environment for the 10th, 50th, and 90th percentile losses. Loss from rain damage included. Left: downtime curve. Right: financial loss curve.

Key limitations

- The wind archetype development assumes certain simplified building geometry, component type, number, location, roof construction type, etc. It might not perfectly represent the individual building in practice
- The component wind-resisting capacities vary significantly based on component condition, manufacturer, construction quality, local requirements. etc. No consistent wind-resisting data is available to date. The archetype considers generic wind zones to determine the wind-resisting capacity based on the design wind speeds. To capture the possible variability, the uncertainty of component capacities was explicitly considered by conducting Monte Carlo simulations. This is consistent with the state-of-the-art approach in wind risk assessment (FEMA 2000, FPHLM 2015, Abdelhady et al. 2021, Alduse et al. 2022)
- The tall building archetype development assumes a simplified wind profile along the building height based on ASCE 7 (ASCE 2022). Wind pressure on tall building components is complex due to local wind effect and dynamic wind effect. Wind tunnel tests or CFD are often needed. Given the general purpose of the study, simplification has been used. Therefore, wind damage and associated consequence results for buildings more than 10 stories tall could be less accurate.
- As only a handful of archetypes were developed to represent the entire building stock, there are simplifications considered in mapping the archetype to represent each building given the building characteristics data available. The individual building characteristics might not be sufficiently captured by the assigned archetype.
- The rule of mapping the individual asset to building archetype is developed to cover generic cases. The rule might not apply to individual building with special characteristics.

References

Abdelhady, A. U., Spence, S. M. J., and McCormick, J. (2021). “A Resilience-Based Assessment of the Performance of Residential Communities Subject to Hurricane Hazard.” Proceedings of International Structural Engineering and Construction, 8(1), doi: 10.14455/ISEC.2021.8(1).RAD-09.

Alduse, B., Pang, W., Tadinada, S.K., and S. Khan. (2022). “A Framework to Model the Wind-Induced Losses in Buildings during Hurricanes.” Wind, 2(1), 87–112, doi: 10.3390/wind2010006.

Alexandre, P.M.; Mockrin, M.H.; Stewart, S.I.; Hammer, R.B.; and Radeloff, V.C. (2015). Rebuilding and new housing development after wildfire. International Journal of Wildland Fire, 24, 138-149. Retrieved from www.fs.fed.us/rm.

American Society of Civil Engineers (ASCE). (2022). Minimum Design Loads for Buildings and Other Structures. ASCE Standard ASCE/SEI 7-22. American Society of Civil Engineer, Reston, US.

Applied Technology Council. (2013). FEMA P-58 Seismic Performance Assessment of Buildings Volume 1 - Methodology. Retrieved from https://femap58.atcouncil.org/documents/fema-p-58/24-fema-p-58-volume-1-methodology-second-edition/file

Armal, Saman, Jeremy R. Porter, Brett Lingle, Ziyan Chu, Michael L. Marston, and Oliver EJ Wing. "Assessing property level economic impacts of climate in the US, new insights and evidence from a comprehensive flood risk assessment tool." *Climate* 8, no. 10 (2020): 116.

Arup. (2013). REDi Rating System: Resilience-Based Earthquake Design Initiative for the Next Generation of Buildings. Retrieved from https://www.arup.com/perspectives/publications/research/section/redi-rating-system

Babrauskas, V; Society of Fire Protection Engineers. (2003). Ignition handbook: Principles and applications to fire safety engineering, fire investigation, risk management and forensics science. Issaquah, WA: Fire Science Publishers.

Bates, P. D., N. Quinn, C. Sampson, A. Smith, O. Wing, and J. Sosa. "Combined modeling of US fluvial, pluvial, and coastal flood hazard under current and future climates." *Water Resources Research* 57 (2021): e2020WR028673.

Blanchi, R.; Leonard, J. 2005. Investigation of Bushfire Attack Mechanisms Resulting in House Loss in the ACT Bushfire 2003. Bushfire CRC Report.

CA State Senate Committee on Insurance. (2021, March 11). Informational Hearing – Wildfires and Insurance: Emerging Issues. California State Senate. Retrieved from sins.senate.ca.gov.

CAL FIRE. (2019). Before, during and after a wildfire. Retrieved from www.fire.ca.gov.

CAL FIRE. (2019). Post-wildfire recovery. Retrieved from www.readyforwildfire.org.

CAL FIRE. (2019). Returning home after a wildfire. Retrieved from www.readyforwildfire.org.

Chandler, M. (2019, July 26). Carr Fire recovery, 1 year later: Why hundreds of homes still haven't been rebuilt. Record Searchlight. Retrieved from www.redding.com.

Emanuel, K., S. Ravela, E. Vivant and C. Risi. 2006: A Statistical-Deterministic Approach to Hurricane Risk Assessment. *Bull. Amer. Meteor. Soc.,* 87, 299–314.

Federal Emergency Management Agency (FEMA). (2000). Multi-hazard Loss Estimation Methodology-Hurricane Model. Federal Emergency Management Agency, Washington, DC.

FEMA. (2020). Hazus-MH Multi-hazard Loss Estimation Methodology: Flood Model. Technical Manual, FEMA Mitigation Division. Retrieved from https://www.fema.gov/sites/default/files/2020-09/fema_hazus_flood-model_technical-manual_2.1.pdf

FEMA. 2023. National Risk Index. hazards.fema.gov/nri

Filkov, A. & Prohanov, S. (2019). Particle tracking and detection software for firebrands characterization in wildland fires. Fire Technology, 817-836.

Florida Public Hurricane Loss Model (FPHLM). (2015). Florida Public Hurricane Loss Model 6.0. Florida International University, Miami, FL.

Flores, Aaron B., Timothy W. Collins, Sara E. Grineski, Mike Amodeo, Jeremy R. Porter, Christopher C. Sampson, and Oliver Wing. "Federally overlooked flood risk inequities in Houston, Texas: Novel insights based on dasymetric mapping and state-of-the-Art flood modeling." *Annals of the American Association of Geographers* 113, no. 1 (2023): 240-260.

Foote, E. I., Liu, J., & Manzello, S. L. (2012). Characterizing firebrand exposure during wildland-urban interface fires. Fire Technology (online), 1-12.

Gourevitch, Jesse D., Carolyn Kousky, Yanjun Liao, Christoph Nolte, Adam B. Pollack, Jeremy R. Porter, and Joakim A. Weill. "Unpriced climate risk and the potential consequences of overvaluation in US housing markets." *Nature Climate Change* 13, no. 3 (2023): 250-257.

Government Operations Agency. (2022). California Open Data Portal: Organizations: CAL FIRE. California Open Data Portal. Retrieved from data.ca.gov/organization/cal-fire.

Gowri K., D.W. Winiarski, and R.E. Jarnagin. PNNL. Infiltration Modeling Guidelines for Commercial Building Energy Analysis. 2009. Available from:

https://www.pnnl.gov/publications/infiltration-modeling-guidelines-commercial-building-energy-analysis

Kasler, D. and Reese, P. (2019, April 11). In Camp Fire, newer houses were much less damaged. KQED. Retrieved from www.kqed.org.

Kearns, Edward J., David Saah, Carrie R. Levine, Chris Lautenberger, Owen M. Doherty, Jeremy R. Porter, Michael Amodeo et al. "The construction of probabilistic wildfire risk estimates for individual real estate parcels for the contiguous United States." *Fire* 5, no. 4 (2022): 117.

Kim, Jungho, Evelyn Shu, Kelvin Lai, Mike Amodeo, Jeremy Porter, and Ed Kearns. "Assessment of the standard precipitation frequency estimates in the United States." *Journal of Hydrology: Regional Studies* 44 (2022): 101276.

Knapp, E.; Valachovic, Y.S.; Quarles, S.L.; and Johnson, N.G. (2021). Factors associated with single-family home survival in the 2018 Camp Fire, California (preprint). Retrieved from https://doi.org/10.21203/rs.3.rs-580864/v1.

Maranghides, A.; McNamara, D.; Mell, W.; Trook, J.; & Toman, B. (2013). A case study of a community affected by the Witch and Guejito Fires Report (NIST Technical Note 1796). NIST, U.S. Department of Commerce. Retrieved from http://dx.doi.org/10.6028/NIST.TN.1796.

Maranghides, A.; McNamara, D.; Vihnanek, R.; Restaino, J.; and Leland, C. (2015). A case study of a community affected by the Waldo Fire (NIST Technical Note 1910). NIST, U.S. Department of Commerce. Retrieved from http://dx.doi.org/10.6028/NIST.TN.1910.

Maranghides, A.; and McNamara, D. (2016). 2011 Wildland Urban Interface Amarillo Fires Report #2 (NIST Technical Note 1909). NIST, U.S. Department of Commerce. Retrieved from http://dx.doi.org/10.6028/NIST.TN.1909.

Maranghides, A.; Mell, W.; Hawks, S.; Wilson, M.; Brewer, W.; Link, E.; Brown, C.; Murrill, C.; and Ashley, E. (2020). Preliminary data collected from the Camp Fire reconnaissance (NIST Technical Note 2128). NIST, U.S. Department of Commerce. Retrieved from https://doi.org/10.6028/NIST.TN.2128.

McAlpine, Steven A., and Jeremy R. Porter. "Estimating recent local impacts of sea-level rise on current real-estate losses: A housing market case study in Miami-Dade, Florida." *Population Research and Policy Review* 37 (2018): 871-895.

McGough, M. (2021, Sept 14). California wildfires: Caldor Fire damage inspection complete; Dixie Fire near million acres. The Sacramento Bee. Retrieved from www.sacbee.com.

McKay, J. (2020, Nov. 18). After Camp Fire, Paradise, CA works on long-term recovery.

Government Technology. Retrieved from www.govtech.com.

Melecio-Vázquez, David, Chris Lautenberger, Ho Hsieh, Michael Amodeo, Jeremy R. Porter, Bradley Wilson, Mariah Pope, Evelyn Shu, Valentin Waeselynck, and Edward J. Kearns. 2023. "A Coupled Wildfire-Emission and Dispersion Framework for Probabilistic $PM_{2.5}$ Estimation" *Fire* 6, no. 6: 220. https://doi.org/10.3390/fire6060220

National Fire Protection Association, Society of Fire Protection Engineers, & Books24x7, Inc. (2002). SFPE handbook of fire protection engineering, third edition (3rd ed.).

Nazare, S.; Leventon, I.; Davis, R. 2021. Ignitability of Structural Wood Products Exposed to Embers During Wildland Fires: A Review of Literature. NIST Technical Note 2153.

Newboles, A. (2020, Sept 27). Cal Fire releases final North Complex damage totals in Butte County. KRCR. Retrieved from krcrtv.com.

Nofal, O., & van de Lindt, J. W. (2020, August). Minimal Building Flood Fragility and Loss Function Portfolio for Resilience Analysis at the Community-Level. Water, 12(2277). doi:http://dx.doi.org/10.3390/w12082277

Orbital Insight. (2019, Oct 15). Measuring impact and recovery of California wildfires. Retrieved from orbitalinsight.com.

Penney, G., Habibi, D., Cattani, M., & Richardson, S. (2020). A handbook of wildfire engineering: guidance for wildfire suppression and resilient urban design.

Pita, G., Pinelli J.P, Cocke, S., Gurley, K., Mitrani-Reiser, J., Weekes, J., and Hamid, S. (2012). “Assessment of hurricane-induced internal damage to low-rise buildings in the Florida Public Hurricane Loss Model.” Journal of Wind Engineering and Industrial Aerodynamics, 104–106, 76–87, doi: 10.1016/j.jweia.2012.03.023

Porter, Jeremy R., Michael L. Marston, Evelyn Shu, Mark Bauer, Kelvin Lai, Bradley Wilson, and Mariah Pope. "Estimating Pluvial Depth–Damage Functions for Areas within the United States Using Historical Claims Data." *Natural Hazards Review* 24, no. 1 (2023): 04022048.

Porter, Jeremy R., Evelyn G. Shu, Mike F. Amodeo, Neil Freeman, Mark Bauer, Ibrahim Almufti, Meg Ackerson, and Jinal Mehta. "Commercial Real-Estate at Risk: An Examination of Commercial Building and Economic Impacts in the United States Using a High-Precision Flood Risk Assessment Tool." *Frontiers in Water* 4 (2022): 875995.

Porter, Jeremy R., Evelyn Shu, Michael Amodeo, Ho Hsieh, Ziyan Chu, and Neil Freeman. "Community flood impacts and infrastructure: Examining national flood impacts using a high precision assessment tool in the united states." *Water* 13, no. 21 (2021): 3125.

Rissel, S. & Ridenour, K. (2013). Ember production during the Bastrop Complex Fire. Fire Management Today, 72(4), 7-13.

Shu, Evelyn G., Jeremy R. Porter, Bradley Wilson, Mark Bauer, and Mariah L. Pope. "The Economic Impact of Flood Zone Designations on Residential Property Valuation in Miami-Dade County." *Journal of Risk and Financial Management* 15, no. 10 (2022): 434.

Solano County. (2020). LNU Lightning Complex Fire. Solano County Office of Emergency Services. Retrieved from www.solanocounty.com.

Sommer, L. (2020, Nov 25). Rebuilding after a wildfire?. NPR. Retrieved from www.npr.org.

State of California. (2022). CAL FIRE: Incidents. CAL FIRE. Retrieved from www.fire.ca.gov/incidents/.

Tedesco, Marco, Steven McAlpine, and Jeremy R. Porter. "Exposure of real estate properties to the 2018 Hurricane Florence flooding." *Natural Hazards and Earth System Sciences* 20, no. 3 (2020): 907-920.

Thomas, J., et al. (2017). Investigation of firebrand generation from an experimental fire: Development of a reliable data collection methodology. Fire Safety Journal, 864-871.

U.S. Army Corps of Engineers. (2009). Louisiana Coastal Protection and Restoration Technical Report. New Orleans, LA: U.S. Army Corps of Engineers.

USDA Forest Service. 2023. Wildfire Risk to Communities. wildfirerisk.org

Vickery, P., Skerlj, P., Lin, J., Tisdale, Jr., L., Young, M., and Lavelle, F. (2006). “HAZUS-MH Hurricane model methodology. II: Damage and Loss Estimation.” Natural Hazards Review, 7(2), 94-103.

Wallingford, N. (2018). Camp incident damage inspection report (CABTU 016737). CAL FIRE. Retrieved from www.nist.gov.

Wilson, Bradley, Jeremy R. Porter, Edward J. Kearns, Jeremy S. Hoffman, Evelyn Shu, Kelvin Lai, Mark Bauer, and Mariah Pope. "High-Resolution Estimation of Monthly Air Temperature from Joint Modeling of In Situ Measurements and Gridded Temperature Data." *Climate* 10, no. 3 (2022): 47.

Wing, Oliver EJ, Andrew M. Smith, Michael L. Marston, Jeremy R. Porter, Mike F. Amodeo, Christopher C. Sampson, and Paul D. Bates. "Simulating historical flood events at the continental scale: observational validation of a large-scale hydrodynamic model." *Natural Hazards and Earth System Sciences* 21, no. 2 (2021): 559-575.

Wing, Oliver EJ, William Lehman, Paul D. Bates, Christopher C. Sampson, Niall Quinn, Andrew M. Smith, Jeffrey C. Neal, Jeremy R. Porter, and Carolyn Kousky. "Inequitable patterns of US

flood risk in the Anthropocene." *Nature Climate Change*12, no. 2 (2022): 156-162.

Wobus, Cameron, Jeremy Porter, Mark Lorie, Jeremy Martinich, and Rachel Bash. "Climate change, riverine flood risk and adaptation for the conterminous United States." *Environmental Research Letters* 16, no. 9 (2021): 094034.

Zen, S., Thomas, J. C., Mueller, E. V., Dhurandher, B., Gallagher, M., Skowronski, N., & Hadden, R. M. (2021). Development of a field deployable firebrand flux and condition measurement system. Fire Technology, 1401-1424.